

## Silicon vacancy related defect in 4H and 6H SiC

E. Sörman, N. T. Son, W. M. Chen, O. Kordina, C. Hallin, and E. Janzén

*Department of Physics and Measurement Technology, Linköping University, S-581 83 Linköping, Sweden*

(Received 18 August 1999)

We report on an irradiation-induced photoluminescence (PL) band in 4H and 6H SiC and the corresponding optically detected magnetic resonance (ODMR) signals from this band. The deep PL band has the same number of no-phonon lines as there are inequivalent sites in the respective polytype. These lines are at 1352 and 1438 meV in the case of 4H and at 1366, 1398, and 1433 meV in the case of 6H. The intensity of the PL lines is reduced after a short anneal at 750 °C. ODMR measurements with above-band-gap excitation show that two spin-triplet ( $S=1$ ) states with a weak axial character are detected via each PL line in these bands. One of these two triplet states can be selectively excited with the excitation energy of the corresponding PL line. These triplet signals can therefore be detected separately and only then can the well documented and characteristic hyperfine interaction of the silicon vacancy in SiC be resolved. Considering the correlation between the irradiation dose and the signal strength, the well established annealing temperature and the characteristic hyperfine pattern, we suggest that this PL band is related to the isolated silicon vacancy in 4H and 6H SiC. The spin state ( $S=1$ ) implies a charge state of the vacancy with an even number of electrons. By combining the knowledge from complementary electron-spin resonance measurements and theoretical calculations we hold the neutral charge state for the strongest candidate.

### I. INTRODUCTION

SiC is a very promising semiconductor for devices that have to work under extreme conditions. Material properties, such as a wide band gap, good thermal conductivity, a relatively high mobility, and high breakdown voltage, make it appropriate for many demanding applications. SiC is the classical example of polytypism, i.e., the material can crystallize in many different but closely related crystal structures. The unit cells of the 4H and 6H polytypes contains  $4 \cdot 2 = 8$  and  $6 \cdot 2 = 12$  atoms, respectively. The various atomic sites in such large unit cells have different configurations of their neighbors. The nearest neighbors are always tetrahedrally oriented but the next-nearest neighbors can either be in a cubic ( $k$ ) or a hexagonal ( $h$ ) configuration. In 4H SiC there is one site of each type ( $h$  and  $k$ ) while in 6H SiC there are one hexagonal and two cubic sites ( $h$ ,  $k_1$  and  $k_2$ ). The two cubic sites differ in the third shell of neighbors.

This paper will dwell on a primary defect in SiC that in this case has been produced by high-energy particle bombardment. If the energy of these particles is high enough, the atoms in the lattice can actually be pushed out of their places. The primary defects created in this way are generally vacancies and interstitials, but in a binary compound like SiC also the antisites can be formed. There is a reason why a good knowledge about primary defects is especially important for SiC. The poor diffusivity of dopants in SiC makes ion implantation a more attractive doping method. The bombardment of the material with heavy ions creates a lot of defects in the material. In contrast to silicon these primary defects in SiC seem to be stable at room temperature<sup>1-4</sup> and some secondary defects (produced during a post-irradiation thermal annealing) are stable at least up to 2000 °C,<sup>5</sup> i.e., they are virtually impossible to get rid of. This group of defects are therefore not only of a great scientific but also of great technological interest, since they have to be dealt with

in any device process that involves ion implantation.

The primary defects are of course also fundamentally interesting. At quite an early stage in semiconductor science (late 1960s and early 1970s) electron-spin resonance (ESR) measurements revealed some of the fascinating microscopic properties of the vacancy in silicon. Less is still known about the vacancy in diamond, but the properties of the negative charge state has been thoroughly analyzed by ESR. The results from silicon and diamond are in one respect strikingly different. While the different charge states of the vacancy in silicon exhibit a strong lattice relaxation, i.e., a dominating Jahn-Teller effect, the vacancy in diamond has the high-spin ground-state characteristic for a dominating spin-spin interaction. The extreme relaxation in silicon even results in a reversing of the expected ordering of the different charge states in the band gap. It is therefore not strange that these two fundamental point defects have served as interesting model cases in the development of defect theories.<sup>6</sup> Since SiC in a way is a mixture of the two, it is now interesting if some of the properties of its vacancies can be investigated.

Despite all the results reported from investigations of primary defects in SiC by methods like ESR, photoluminescence (PL) and deep-level transient spectroscopy (DLTS), the knowledge about them is far from as developed as silicon. Some experimental knowledge about the carbon and silicon vacancy has, however, been gained. In this paper we will mainly refer back to the extensive ESR investigations on 3C,<sup>1,4</sup> 6H,<sup>3,4</sup> and 4H (Ref. 7) SiC, of what is now accepted to be the ESR signal from the negatively charged silicon vacancy. The deep PL band, that we here will claim to be related to the silicon vacancy, can be observed from as-grown Lely crystals and was thoroughly investigated already during the 1970s. The characteristics of the band was then reported for the 6H,<sup>8,9</sup> 15R,<sup>8,9</sup> and 33R (Ref. 10) polytype. (Historical remark: It was then usually referred to as the *abc* band.) The most thorough work is the PL study by Hagen

and Kemenade where they convincingly show that this PL band is not impurity related.<sup>9</sup> Since all the different authors were lacking information from magneto-optical or magnetic resonance experiments, they were not able to draw the conclusions about the origin of these PL signals that we have been able to. The early work on radiation induced defects in SiC was reviewed by Choyke in 1977.<sup>11</sup>

In optically detected magnetic resonance (ODMR) one measures the fractional change in the luminescence, that a magnetic resonance in an excited state of a local defect induces. The technique is in a sense complementary to the ESR technique, since the short-lived excited states of defects are investigated, rather than the more permanently populated ground states. If the radiation-induced defects in SiC form efficient recombination centers, ODMR is the appropriate method to investigate these.

## II. SAMPLES AND EQUIPMENT

The samples used were all high-quality epitaxial layers, grown by chemical vapor deposition. The nitrogen concentration in these samples is in the  $10^{14} \text{ cm}^{-3}$  range.<sup>12</sup> In order to produce the primary defects, the samples were irradiated with 2.5 MeV electrons in doses ranging from  $10^{15}$  to  $10^{18} \text{ cm}^{-2}$ .

For the X-band ( $\approx 9.22 \text{ GHz}$ ) ODMR experiments we used a modified Bruker ER-200D electron-spin resonance spectrometer equipped with a cylindrical  $\text{TE}_{011}$  microwave cavity with optical access. UV-light from an argon-ion laser was used for above band gap excitation, while a tunable Ti:sapphire laser was used for resonant excitation of the studied defects. In the ODMR experiments the luminescence either passed appropriate optical filters or a 0.25 m monochromator before detection with a liquid-nitrogen-cooled germanium photodiode (North Coast). Most of the photoluminescence (PL) experiments were carried out using a 0.46 m grating monochromator equipped with a silicon charge-coupled device (CCD) detector. The sample temperature could be varied from room temperature down to liquid-helium temperature in both the ODMR and the PL experiments.

## III. PHOTOLUMINESCENCE

There are several PL bands in SiC, both relatively shallow and deep, that are associated with radiation damage. We will discuss the particular irradiation induced bands in 4H and 6H SiC, shown in Fig. 1. The no-phonon lines are sharp (the linewidth is about 0.4 meV in the best samples) and the number of them is, as expected, the same as the number of inequivalent sites in the 6H (three sites) and 4H (two sites) polytype. We will in this paper argue for a correspondence between the bands from the two polytypes and will therefore simply label the lines in the same way. We will refer to the 1433-, 1398-, and 1366-meV lines in 6H as the V1, V2, and V3 lines and the 1438- and 1352-meV lines in 4H as the V1 and V2 lines. Table I contains a summary of all the line positions discussed in the paper.

A short anneal at  $750^\circ\text{C}$  decreases the intensity of the PL band dramatically, in both polytypes. This temperature is identical to the annealing temperature of the silicon vacancy

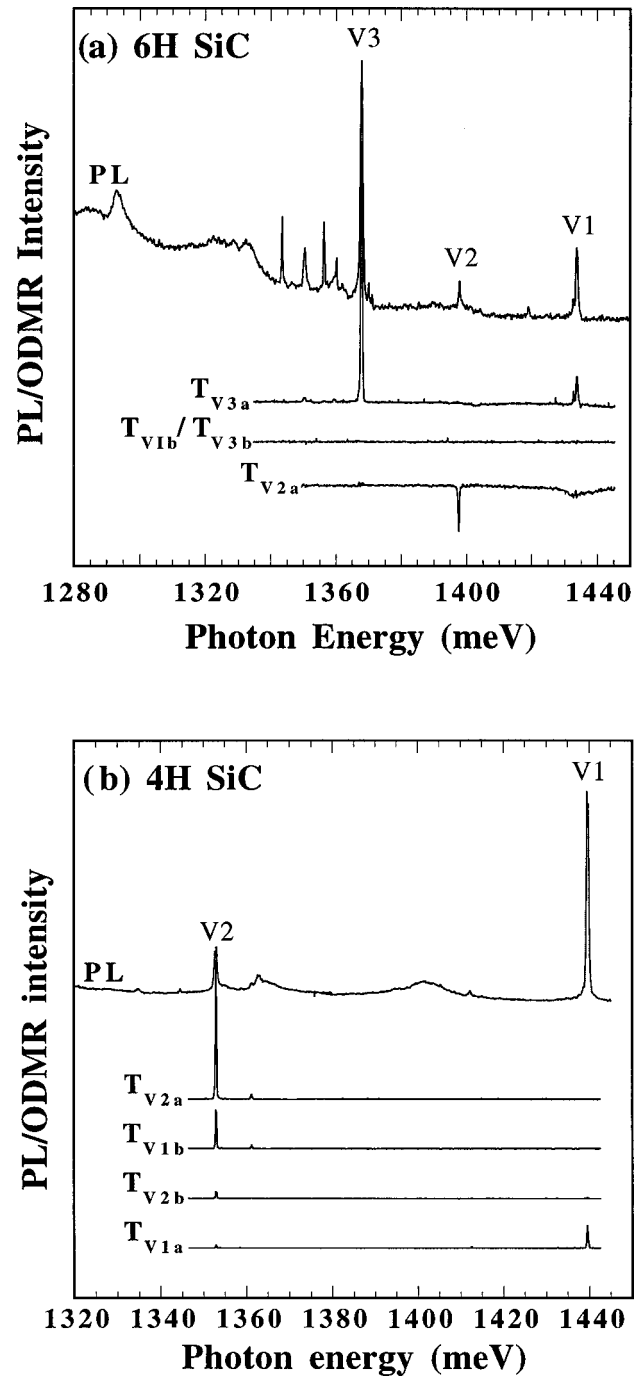


FIG. 1. At the top the deep PL band and below the excitation spectrum of the various ODMR signals that are detected from the PL band for the 6H (a) and 4H (b) polytypes.

in irradiated 3C and 6H SiC.<sup>1,3</sup>

The intensity of the V lines increases with irradiation dose up to  $10^{17} \text{ cm}^{-2}$  but not further. At higher doses, there is a general decrease in the luminescence intensity. The reason is probably that the nonradiative channels that are also induced by the irradiation become more important at the highest doses. The intensity of the band is generally quite insensitive to the impurity content of the sample as long as it is *n* type. The signal from *p*-type samples is consequently much weaker.

In agreement with the early results on 6H Lely crystals<sup>8</sup>

TABLE I. Labels, energies, zero-field splitting of the corresponding triplet state ( $D$ -value), and corresponding defect sites of the no-phonon PL lines in the 4H and 6H polytype.

Polytype	No-phonon line label, energy (meV)	Corresponding $D$ -value ( $10^{-8}$ eV)	Corresponding inequivalent site
6H	V1 1433	11.4	$k_1$
	V2 1398	53.1	$h$
	V3 1366	11.4	$k_2$
4H	V1 1438	1.8	$k$
	V2 1352	28.8	$h$

the intensity of the PL lines in 6H is almost constant up to 60 K and decreases at higher temperatures. At 170 K the lines are still detectable, but very weak. The intensity of the PL lines in 4H seems always to be weaker than in 6H. For the 4H polytype, the intensity of the lines starts to fall off already at 30 K and is reduced to one-quarter of their strength at 60 K.

#### IV. ODMR

The ODMR spectrum, shown in Fig. 2, can be detected via the PL band discussed above. Separating the spectrum into its components, we found it to consist of twice as many ODMR signals as there are PL lines. All signals are marked and labeled in the illustration and the fact that only five and not six signals are resolved in the case of 6H will be discussed more below. The ODMR signals all consist of two lines whose splitting vary in the relatively simple fashion indicated in Fig. 3, when the crystal is rotated in the magnetic field. The splitting is only governed by the angle between the magnetic field and the  $c$  axis of the crystal. This angular dependence of the ODMR signals is characteristic for a spin-triplet state ( $S=1$ ) with axial symmetry. To clarify this statement, an illustration that schematically describes the spin triplet is included as Fig. 4. There it is also indicated how the allowed microwave-induced transitions  $\Delta M = \pm 1$  will cause a change in the luminescence intensity if there is a difference in the recombination rate from the magnetic sublevels. This is then the mechanism causing the ODMR signal. Observe that the splitting of the ODMR signal is directly related to the zero-field splitting of the triplet. In a simple case like this, the angular dependence can be fitted by the following expression:<sup>13</sup>

$$B = \frac{1}{g\mu_B} \left( h\nu \pm \frac{D}{2} [3(\cos\theta)^2 - 1] + AM_I \right).$$

Here  $g$  is the gyromagnetic ratio,  $\mu_B$  is the Bohr magneton,  $D$  is the zero-field splitting of the magnetic sublevels,  $A$  describes isotropic hyperfine interaction and  $\theta$  is the angle between the  $c$  axis of the crystal and the magnetic field. The parameters of such a function can be fitted to all the different ODMR signals. The resultant fitting and the corresponding parameters are shown in Fig. 3 and Table II, respectively. Since no hyperfine structure could be resolved in this experiment, the last term was not included in the fit. It will, however, come in use later.

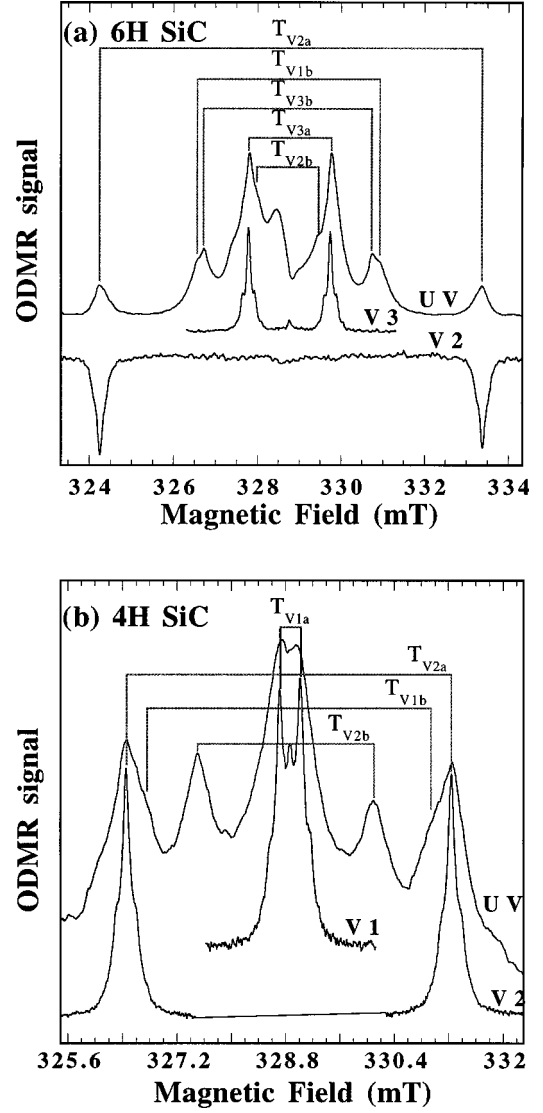


FIG. 2. At the top the ODMR spectrum with above-band-gap excitation and below with selective excitation with the energies of the no-phonon lines for the 6H (a) and 4H (b) polytypes. The magnetic-field direction is in both cases  $10^\circ$  off the  $c$  axis of the crystal. The naming of the ODMR signals are introduced.

#### A. Spectral dependence

To sort out the correspondence between the different ODMR signals and the PL lines, ODMR was measured from each PL line separately. Even though great noise problems, because of the low signal strength, were encountered, it is hopefully apparent from Fig. 5 that two ODMR signals are always detected from each PL line.

When inspecting the results from the 6H polytype observe that, since the V1 line has phonon replicas close to both the V2 and V3 line, the ODMR spectra of the V1 line is also partly detected in the V2 and V3 line spectrum. If this contribution is subtracted from the V3 line spectrum a strong  $T_{V3a}$  signal still remains, i.e., both the V1 and V3 lines give contributions to the  $T_{V3a}$  signal that are not distinguishable, at least not with the resolution of our spectrometer. For the 4H polytype note that since the V1 line has phonon replicas very close to the V2 line, the ODMR signals from this line are partly detected when the V2 line is selected.

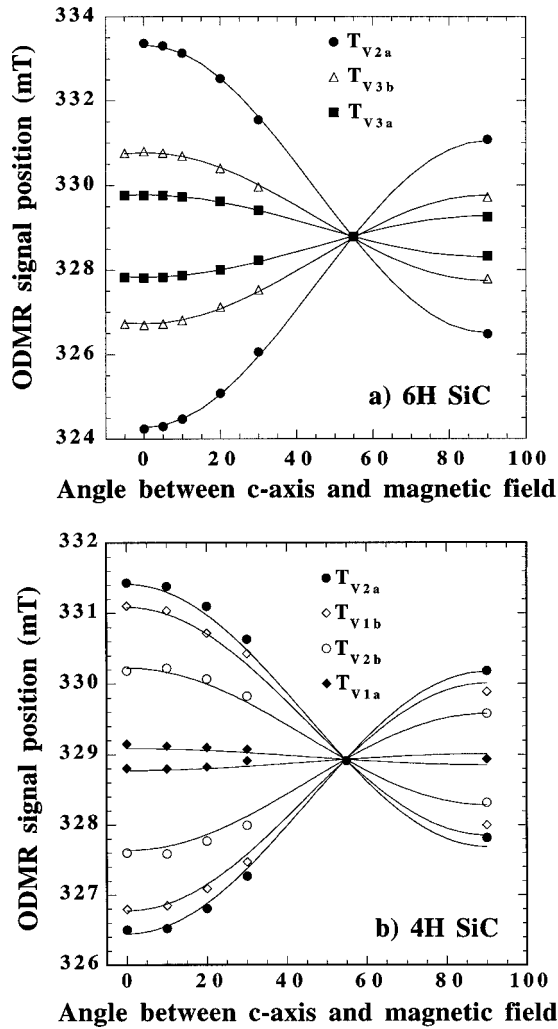


FIG. 3. Angular dependence of the ODMR signals detectable with above-band-gap excitation for the 6H (a) and 4H (b) polytypes. The lines indicate the fits that are obtained with the parameters in Table II.

### B. Resonant excitation

If the magnetic field is locked at the position of one of the ODMR signals and the excitation energy is scanned through the energy region of the PL band, as in Fig. 1, it becomes apparent that some of these triplet states can be excited resonantly. The resonance energies are in fact identical to the energies of the no-phonon lines in the PL spectra and there is only one triplet state corresponding to each PL line. The concluded correlation between the PL lines and the ODMR signals from this experiment agrees with the results from the spectral dependence experiment described in the preceding section. This experiment gives in addition a direct one-to-one correspondence between some of the triplet states and the PL lines. It should now be understandable why the ODMR signals are named like they are. Apart from the  $T$  which stands for triplet, the  $V1$ ,  $V2$ , or  $V3$  indicates the correspondence to the PL lines and the  $a$  or  $b$  marks if the triplet state is resonantly excitable (a) or if it is only detected with above band-gap excitation (b).

The directly corresponding ODMR signals (will be referred to as primary triplets) can, as indicated in Fig. 2, be detected separately if this resonant excitation is used. It then

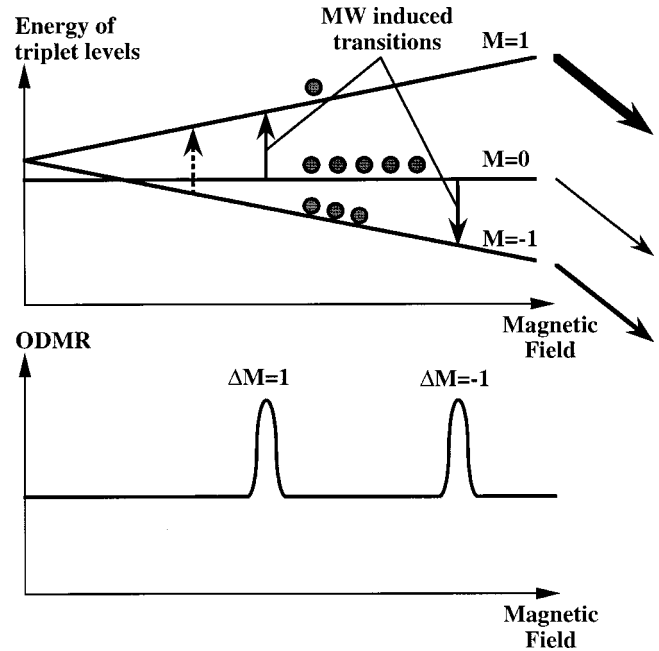


FIG. 4. Schematic illustration indicating the origin of the ODMR in the spin-triplet case. The width of the arrow at each sublevel is scaled with the recombination rate.

becomes possible to resolve the hyperfine structure of these ODMR signals. Each resonance line has a symmetric pair of inner and outer satellites that are split by 0.30 and 0.60 mT, respectively. If the hyperfine structure is fit with Lorentzian functions with identical linewidths (Fig. 6), the intensity of the inner and outer satellites are in general found to be 27% and 4% of the central line. The analysis of the  $T_{V1a}$  signal in 4H is more difficult than the others, since the two hyperfine structures interfere even at the angle where the splitting of the two resonances is the largest [Fig. 2(b)]. Apart from the problem that it is very hard to extract a relative intensity for the outer satellites the other parameters (splitting and intensity of the inner satellites) are within the accuracy identical to the other primary triplet states. The hyperfine structure is isotropic and can therefore be represented by a simple  $A$  value in the spin Hamiltonian.

One comment on the 4H spectra [Fig. 1(b)]: The weak line at 1.36 eV in the two first-excitation spectra corresponds to another near-lying triplet signal. This signal does, however, not have the same characteristic hyperfine splitting as the  $T_{V1a}$  and  $T_{V2a}$  signals.

No resonant excitation is possible for the other triplet states (type  $b$ ) in this energy range. For 4H excitation was tried up to 1.46 eV and for 6H all the way up to 1.77 eV.

## V. DISCUSSION

### A. Identification

As an introduction we discuss some of the properties of a point defect at a silicon site in the SiC lattice and the earlier work done on the silicon vacancy in SiC. The hyperfine interaction of a point defect at a silicon site, with the four nearest-neighbor (NN) carbon atoms, is expected to be the strongest (the interaction strength governs the splitting). The satellites are very weak though, since the natural abundance

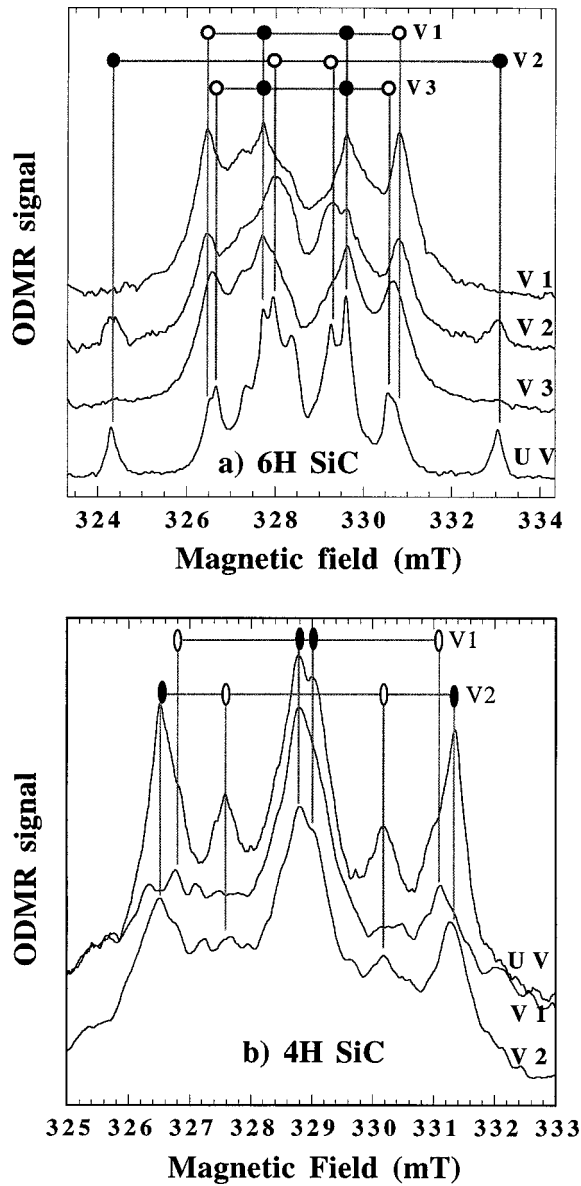


FIG. 5. The ODMR spectrum when the whole PL band is detected and when each PL line is detected individually for the 6H (a) and 4H (b) polytype. Type-*a* triplets have filled markers while type *b* have open markers.

of the nuclear-spin active isotope  $^{13}\text{C}$  ( $I=1/2$ ) is only 1.1%. Among the 12 next-nearest-neighbor (NNN) silicon atoms, 4.7% are of the nuclear-spin active isotope  $^{29}\text{Si}$  ( $I=1/2$ ). If the wave function of the defect is extended enough to interact also with the NNN silicon atoms and if the interaction with these NNN's is assumed to be equivalent, the hyperfine structure will consist of pairs of hyperfine satellites with an energy splitting of  $A$ ,  $2A$ ,  $3A$ , etc. These pairs then corresponds to one, two, three, etc., nuclear-spin active  $^{29}\text{Si}$  atoms among the 12 NNN's. The probability for these NNN constellations is decreasing rapidly with the number of  $^{29}\text{Si}$  and is already neglectable for three  $^{29}\text{Si}$ . In short, such NNN-related hyperfine satellites are expected to be equidistant, have smaller splittings than the NN-related satellites, and the statistical prediction of the intensity ratio of the five strongest lines are 3.7-28-100-28-3.7.

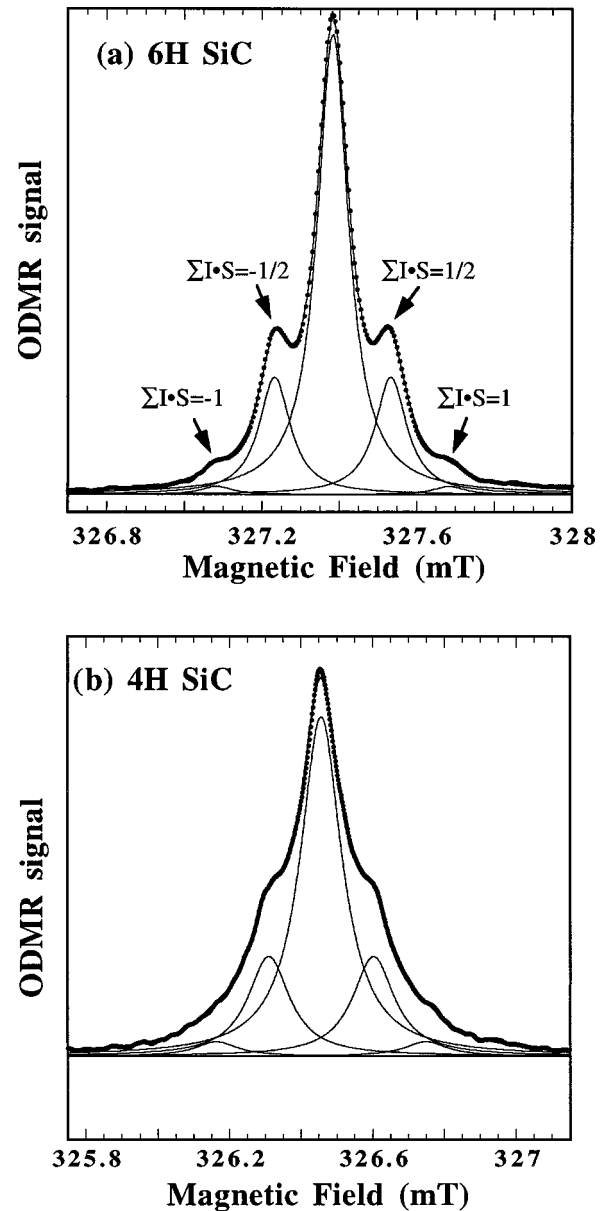


FIG. 6. An enlargement of the hyperfine structure of the  $T_{V3a}$  in 6H and the  $T_{V2a}$  signal in 4H, both fitted with five pairwise coupled and equidistant Lorentzians. The lines indicate the fitted curve and its subcomponents and the points are the experimental data.

An isotropic signal from an effective  $S=1/2$  defect that has the expected hyperfine interaction with both the carbon NN's and the silicon NNN's, but no trace of hyperfine interaction with the defect itself, has been reported for irradiated 3C,<sup>1</sup> 6H,<sup>3</sup> and 4H (Ref. 7) SiC. Considering the creation efficiency, the spin state, and all the aspects of the hyperfine interaction, the authors<sup>2</sup> proposed a negatively charged silicon vacancy model ( $V_{\text{Si}}^-$ ). This model has now gained acceptance. The number of NNN's are 12 in all three polytypes, so if the interaction strength with the individual NNN is almost equal, the geometrical configuration of the NNN shell (there are two different in 6H and 4H) does not have any influence on the NNN hyperfine structure. This would explain why the NNN hyperfine structure seems insensitive to both the defect site and to polytype. Recent electron nuclear double resonance (ENDOR) measurements on the

4H polytype indicate that the true spin state of the  $V_{\text{Si}}^-$  is  $S = \frac{3}{2}$ , as expected for an undistorted center.<sup>7</sup> That this charge state should have a high-spin ground state was already predicted in the calculations by Larkins and Stoneham in 1970 (Ref. 14) and has later been confirmed by more refined calculations.<sup>15,16</sup>

The intensity ratios and the splitting of the hyperfine structure of the signals from the  $V_{\text{Si}}^-$  are indeed very similar to what we observe for the  $T_{V1a}$ ,  $T_{V2a}$ , and  $T_{V3a}$  centers. To be more specific, the intensity ratios and the equidistance of the satellites are as expected for interaction with a silicon NNN shell and the interaction strength is, in fact, the same as for the silicon vacancy signal ( $V_{\text{Si}}^-$ ) discussed above. None of the common impurities in SiC, such as N, Al, B, Ti, V, or H, would cause such a hyperfine pattern. The continuous increase of the ODMR and PL signal strength with irradiation dose and the insensitivity of the signal strength to the impurity content of the sample also indicate that the signal is related to primary defects rather than impurities. In addition, the annealing temperature of the PL band agrees well with the observed annealing temperature in the various ESR works on the  $V_{\text{Si}}^-$  signal.<sup>1,3</sup>

A quick review of the argumentation chain: The correspondence between the number of PL lines and the number of inequivalent sites is characteristic for a recombination at a localized defect (that in general is sensitive to the immediate surroundings). The correlation of the signal strength with irradiation dose but not with sample purity is typical for a primary defect. The annealing temperature of the PL band and the very characteristic hyperfine structure of the ODMR signal strongly favors the silicon vacancy among the primary defects.

### B. Electronic structure

The similarities between the hyperfine pattern of our primary triplet states  $T_{V1a}$ ,  $T_{V2a}$ , and  $T_{V3a}$  and the  $V_{\text{Si}}^-$  signal, the absence of central hyperfine interaction, and the relatively high symmetry indicate that these triplet states are related to the isolated silicon vacancy. The triplet state, however, calls for another set of particles around the vacancy, since the odd number of electrons at  $V_{\text{Si}}^-$  cannot form a spin-triplet state. The hyperfine-interaction strength of the triplets are very similar to that of the  $V_{\text{Si}}^-$  signal. It is well known that the interaction strength of the triplet particles is the average of the individual particles interaction strength.<sup>17</sup> This then indicates that we are dealing with another charge state of the vacancy where the localized electrons, which give rise to the observed spin triplets, interact with the NNN's in a similar way as the electrons of the  $V_{\text{Si}}^-$  state. Only a charge state with an even number of spin-active particles can form a triplet state. Calculations on the 4H polytype indicate that the doubly positive ( $V_{\text{Si}}^{+2}$ ), the neutral ( $V_{\text{Si}}^0$ ), and the doubly negative charge state ( $V_{\text{Si}}^{2-}$ ) all have a level in the band gap.<sup>15,16</sup> ESR signals from the ground states of any of these other charge states of the  $V_{\text{Si}}$  have not been reported. From a theoretical point of view only the doubly positive charge state is expected to have a nonparamagnetic ground state, i.e., a singlet state, while the other two are expected to have triplet ground states.<sup>15,16</sup> The doubly positive charge state is, however, only expected to be stable when the Fermi level is very

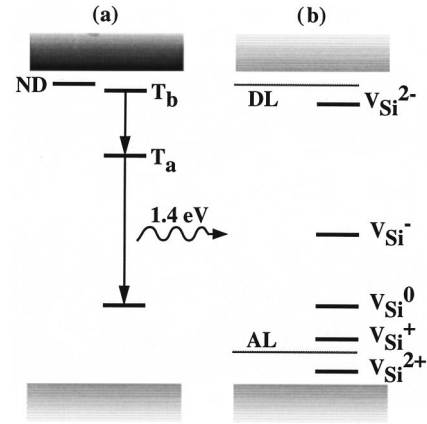


FIG. 7. Schematic illustration showing the suggested electronic transitions related to the PL and ODMR signals (a) and the approximate positions of the various charge states of the silicon vacancy (b) implied by the combination of theoretical calculations and our ESR results. ND stands for nitrogen donor, AL for acceptor level, and DL for donor level.

close to the valence band. Conversion to the next charge state is expected to occur already  $124^{15}/70^{16}$  meV above the valence band, i.e., well below any acceptor level. The marked difference in PL intensity between *n*- and *p*-type samples indicates that the charge state we are dealing with has its stability interval above the acceptor levels, i.e., it is probably not the doubly positive charge state. This far, the neutral and doubly negative charge states are therefore the strongest candidates. In our proposed model, the  $V1$ ,  $V2$ , and  $V3$  PL lines would then originate from internal transitions from an excited state of one of these charge states of the  $V_{\text{Si}}$ . The different PL lines can then be attributed to transitions at the inequivalent sites in the SiC lattice. Note that an excitonic model where a hole is coulombically attracted to the negatively charged vacancy is not applicable, since such a hole would be much less localized than the primary bound electron and therefore would cause a weaker hyperfine interaction than the observed.

From the ODMR results alone it is not possible to sort out the question about the charge state of the  $V_{\text{Si}}$ . The model requires that the excited states from which the PL and ODMR signals originate lie in the band gap. The corresponding ground state must therefore, as indicated in Fig. 7(a) be located at least 1.44 eV (6H) below the conduction band. In the illustration it is also assumed that the type-*b* triplets are related to higher excited states. The ground states then actually have to be located more than 1.77 eV (6H) below the conduction band, since the excitation experiments show that this energy is not sufficient to excite the type-*b* states.

To get more information about the positions of these vacancy levels in the band gap we performed ESR measurements on a series of *n*-type samples with different irradiation doses, i.e., samples that are expected to have a systematic variation of the Fermi level. The ESR signal from the nitrogen donor could be detected in all the samples, indicating that the Fermi level is still close to the donor level even in the samples with the highest dose. On the other hand, it was only from the sample with the highest irradiation dose ( $10^{18}$  cm<sup>-2</sup>) that the well-known ESR signal from the  $V_{\text{Si}}^-$  state could be detected. If the dose is lower, as for the

TABLE II. The spin Hamiltonian parameters of the triplet states detectable with above-band-gap excitation and the correspondence to the PL lines for the two polytypes. Some results from the literature are also included for comparison. The asterisks indicate higher accuracy since the  $T_{V1a}$ ,  $T_{V2a}$ , and  $T_{V3a}$  signals can be studied separately.

Polytype	Triplet states	$g_{\parallel} \pm 0.002$	$g_{\perp} \pm 0.002$	$D (10^{-8} \text{ eV}) \pm 0.2$	$A (10^{-8} \text{ eV})$	PL line label
4H	$T_{V1a}$	2.004*	2.004*	1.8*	3.5	V1
	$T_{V1b}$	2.004	2.004	25		V1
	$T_{V2a}$	2.004*	2.004*	28.8*	3.5	V2
	$T_{V2b}$	2.004	2.004	15		V2
6H	$T_{V1a}/T_{V3a}$	2.0035	2.0037	11.4		V3,V1
	$T_{V1b}$	2.0037	2.0041	25.5		V1
	$T_{V2a}$	2.0035	2.0038	53.1	3.5	V2
	$P3^a$	2.0026	2.0031	53.3	3.5	
	$T_{V2b}$	$\approx 2.004$	$\approx 2.004$	$\approx 8.2$		V2
	$T_{V3a}$	2.0037*	2.0038*	11.4*	3.5	V3
	$P5^a$	2.0026	2.0031	11.2	3.7	
	$T_{V3b}$	2.0038	2.0039	23.7		V3

<sup>a</sup>Reference 21.

samples that give the strongest ODMR signals ( $10^{17} \text{ cm}^{-2}$ ), there is no trace of this signal. As schematically shown in Fig. 7(b), this indicates that the next stable charge state above the well-known  $V_{\text{Si}}^-$  state is located closely below the nitrogen donor level and that this state is ESR inactive. Since there are no indications of strong lattice distortion, we expect a normal sequence of energy levels (no negative- $U$  behavior). This above-lying state then hosts more electrons (two or more). In perspective of the requirements from the suggested model, it is then very improbable that this above-lying state is the origin of the PL and ODMR signals, since the excited states would then have to be far up in the conduction band. This argument finally leaves us with the neutral charge state as the most probable origin.

Working with the strongest signal (the  $T_{V3a}$  in 6H), we have also been able to detect weak satellites (0.5–1 %) with the higher interaction strength expected for NN's, but we have not been able to study the full angular dependence of these satellites like Itoh and his co-workers have done for  $V_{\text{Si}}^-$  in 3C SiC.<sup>6</sup> Because of the directed character of the four bonds, the hyperfine satellites from the individual NN's are separated at most angles. The expected intensity from a single carbon-related satellite is then only 0.55% of the central peak. For the 6H polytype, data for the  $V_{\text{Si}}^-$  is only published with the magnetic field along the  $c$  axis of the crystal.<sup>3</sup> In this direction the hyperfine-interaction strength of our signals is about 30% weaker. Comparing with the spin-active electrons of  $V_{\text{Si}}^-$  this then shows that the electrons in the excited state of  $V_{\text{Si}}^0$  have a slightly weaker interaction with the NN shell but a similar interaction with the NNN shell.

In the 6H crystal there are three inequivalent sites. Two have a cubic configuration of the NNN shell, but differ in the third-NN shell (these are usually called the  $k_1$  and  $k_2$  sites) and one has a hexagonal configuration of the NNN shell ( $h$ ). It can be expected and it has also been shown for substitutional titanium and vanadium in SiC (Refs. 18 and 19) that a defect at a hexagonal site experiences a stronger axial crystal field than one at a cubic site. The triplet states from the V1

and V3 lines in 6H are so similar that they cannot be distinguished from one another. The triplet states from the V2 lines have a stronger axial character than those from the V1 lines in both 4H and 6H. To be more specific, the zero-field splitting of the magnetic sublevels of the V2 triplets is 15 times larger in 4H and 5 times larger in 6H. Considering the 6H polytype, this would then indicate that the V1 and V3 lines are from the cubic sites while the V2 line is from the hexagonal one. When the two polytypes are compared, it is reasonable to assume that the two lines, which both have a much stronger axial character of their corresponding ODMR signals, should correspond to the hexagonal defect site. Since the energetical ordering of the PL lines is expected to be the same in the two polytypes<sup>20</sup> the two V1 lines should correspond to similar cubic sites. The fact that the  $k$  site in 4H mostly resembles the  $k_1$  site in 6H finally enables us to suggest the relations between the PL lines and the inequivalent sites indicated in Table I.

### C. Comparison with previously published results

Judging from the reported energy positions of the non-phonon lines,<sup>8</sup> the PL spectrum discussed here was already observed in 1973 by Gorban *et al.*<sup>8</sup> in as-grown 6H SiC samples. Because of the similarity with the PL band that was soon shown to correspond to titanium, they were led into speculations around various transition metals. This issue was later resolved by Hagen and Kamenade in a very thorough paper that convincingly showed that the band was not related to any common impurity.<sup>9</sup> Both these research groups were lacking the vital pieces of information extractable from magnetic resonance experiments.

As can be seen in Table II, the spin Hamiltonian parameters ( $g$ ,  $D$ , and  $A$ ) of  $T_{V2a}$  and  $T_{V3a}$  are strikingly similar to those of the  $P3$  and  $P5$  centers that Vainer and Il'in observed by photoinduced ESR from thermally quenched and annealed 6H SiC samples.<sup>21,22</sup> At first glance there is a dif-

ference in the intensities of the hyperfine structure, but taking a closer look there seems to be a misleading mistake done in one of the figure captions. Bearing this in mind, it might well be that the hyperfine structure actually is very similar to what we observe. The  $P3$  and  $P5$  are then probably the same defects as the  $T_{V2a}$  and  $T_{V3a}$ . Their analysis of the hyperfine intensities seems too approximate and leads them to explain the  $P3$ ,  $P5$ , and most of the other defects that they observe with models consisting of an interacting silicon and carbon vacancies.

## VI. SUMMARY

We report on a deep PL band in 6H and 4H SiC with three no-phonon lines at 1366 ( $V3$ ), 1398 ( $V2$ ), and 1433 ( $V1$ ) meV in 6H and two at 1352 ( $V2$ ) and 1438 ( $V1$ ) in 4H. The intensity of the bands is dramatically reduced after a 750 °C anneal. Two different spin-triplet states can be detected from each PL line by ODMR. These triplet states all have axial symmetry,  $g$  values close to 2.004, and relatively small  $D$  values. Spectral decomposition and excitation experiments show that each no-phonon line can be associated with one specific triplet state. These directly related triplet states can be studied separately with resonant excitation. Only then is the well documented hyperfine interaction of the silicon vacancy in SiC resolvable. The fact that these signals show up after high-energy particle bombardment, the insensitivity of the intensity to the sample purity, the annealing

behavior, all the aspects of the hyperfine interaction, the number of PL lines/triplet states, and the grouping of the triplet character have led us to suggest that the triplet signals are from the isolated silicon vacancy. The well known  $V_{Si}^-$  state that is observed in ESR experiments cannot with its odd number of electrons form a spin triplet. Both the higher and lower electronic occupancies are possible candidates and from ODMR results alone it is not possible to do a final assignment. Since complementary ESR measurements on the 6H polytype indicate that the higher occupancy states are located too close to the conduction band, the  $V_{Si}^0$  or the  $V_{Si}^{2+}$  state are more probable. Theoretical calculations indicate that the doubly positive charge state has a stability interval that is too close to the valence band to explain the large difference in PL intensity between  $n$ - and  $p$ -type samples. The no-phonon lines, observed in PL, would then originate from internal transitions from an excited state of  $V_{Si}^0$  at the inequivalent sites in 4H and 6H SiC. A comparison of the character of the triplet states between the polytypes indicates that the  $V2$  lines correspond to the hexagonal sites and the  $V1$  and  $V3$  to the cubic sites.

This would then be the first time that a PL signal from the silicon vacancy is identified. The localization of the spin-active electrons is similar to the negative charge state, but in contrast to this state, both the PL and ODMR signals from the inequivalent sites can be resolved and associated with the respective site.

- 
- <sup>1</sup>H. Itoh, M. Yoshikawa, I. Nashiyama, S. Misawa, H. Okumura, and S. Yoshida, *IEEE Trans. Nucl. Sci.* **37** (6), 1732 (1990).
- <sup>2</sup>H. Itoh, M. Yoshikawa, I. Nashiyama, S. Misawa, H. Okumura, and S. Yoshida, *J. Electron. Mater.* **21**, 707 (1992).
- <sup>3</sup>Jürgen Schneider and Karin Maier, *Physica B* **185**, 199 (1993).
- <sup>4</sup>First reported by L. A. de S. Balona and J. H. N. Loubster, *J. Phys. C* **3**, 2344 (1970). The F spectrum is undoubtedly the ESR signal from the  $V_{Si}^-$ .
- <sup>5</sup>Yu. A. Vodakov, G. A. Lomakina, E. N. Mokhov, M. G. Ramm, and V. I. Sokolov, *Fiz. Tekh. Poluprovodn.* **20**, 2153 (1986) [*Surf. Sci.* **20**, 1347 (1986)].
- <sup>6</sup>See, for example, *Point Defects in Semiconductors II*, J. Bourgoin and M. Lanoo (Springer-Verlag, Berlin, 1983).
- <sup>7</sup>T. Wimbauer, D. Volm, B. K. Meyer, A. Hofstätter, and A. Scharman, in *Proceedings of the 23rd International Conference on the Physics of Semiconductors* (World Scientific, Singapore, 1996), p. 2645.
- <sup>8</sup>I. S. Gorban and A. V. Slobodyanyuk, *Fiz. Tverd. Tela* (Leningrad) **15**, 789 (1973) [*Sov. Phys. Solid State* **15**, 548 (1973)].
- <sup>9</sup>S. H. Hagen and A. W. C. van Kemenade, *J. Lumin.* **9**, 9 (1974).
- <sup>10</sup>I. S. Gorban and A. V. Slobodyanyuk, *Fiz. Tverd. Tela* (Leningrad) **16**, 1789 (1974) [*Sov. Phys. Solid State* **16**, 1163 (1974)].
- <sup>11</sup>W. J. Choyke, in *Proceedings of the International Conference on Radiation Effects in Semiconductors* (Institute of Physics and Physical Society, London, 1977), p. 58.
- <sup>12</sup>O. Kordina, A. Henry, J. P. Bergman, N. T. Son, W. M. Chen, C. Hallin, and E. Janzén, *Appl. Phys. Lett.* **66**, 1373 (1995).
- <sup>13</sup>See, for example, J. E. Pake, *Paramagnetic Resonance* (Benjamin, New York, 1962).
- <sup>14</sup>F. P. Larkins and A. M. Stoneham, *J. Phys. C* **3**, L112 (1970).
- <sup>15</sup>L. Torpo (private communication).
- <sup>16</sup>A. Zywiets, J. Furthmüller, and F. Bechstedt, *Phys. Rev. B* **59** (23), 15 166 (1999).
- <sup>17</sup>W. M. Chen, B. Monemar, and M. Godlewski, *Defect Diffus. Forum* **62/63**, 133 (1989).
- <sup>18</sup>K. M. Lee, Le Si Dang, and G. D. Watkins, *Phys. Rev. B* **32**, 2273 (1985).
- <sup>19</sup>K. Maier, H. D. Müller, and J. Schneider, *Mater. Sci. Forum* **83-87**, 1186 (1992).
- <sup>20</sup>That the ordering of the PL lines is kept between the polytypes is a reasonable assumption. It has been shown to be valid for some transition metal systems in SiC (see Refs. 18 and 19).
- <sup>21</sup>V. S. Vainer and V. A. Il'in, *Fiz. Tverd. Tela* (Leningrad) **23**, 3659 (1981) [*Sov. Phys. Solid State* **23**, 2126 (1981)].
- <sup>22</sup>V. S. Vainer, V. I. Veigner, V. A. Il'in, and V. F. Tsvetkov, *Fiz. Tverd. Tela* (Leningrad) **22**, 3436 (1980) [*Sov. Phys. Solid State* **22**, 2011 (1980)].